Polymer Chemistry

PAPER

View Article Online
View Journal | View Issue

Cite this: *Polym. Chem.*, 2017, **8**, 2806

Highly thermal conductive resins formed from wide-temperature-range eutectic mixtures of liquid crystalline epoxies bearing diglycidyl moieties at the side positions†

Youngsu Kim,‡[a,c] Hyeonuk Yeo,‡[a] Nam-Ho You,[a] Se Gyu Jang,[a] Seokhoon Ahn,[a] Kwang-Un Jeong,[b] Seung Hee Lee[c] and Munju Goh *[a]

Received 14th February 2017,
Accepted 31st March 2017

DOI: 10.1039/c7py00243b

rsc.li/polymers

To develop advanced thermally conductive epoxy resins with liquid crystallinity, three novel liquid crystalline epoxies (LCEs) were synthesized *via* the substitution of phenylcyclohexyl (PCH) mesogenic moieties into the 2,5 positions of diglycidyl terephthalate. Mesomorphic properties of LCEs were evaluated by differential scanning calorimetry (DSC), polarized optical microscopy (POM), and X-ray diffraction (XRD). All LCEs exhibited an enantiotropic smectic phase on heating and cooling. Remarkably, the smectic phase with a wide temperature range of 98–145 °C was observed for the eutectic mixtures of a family of stable smectic LCEs. The selection of optimum curing agents, compositions of LCEs and curing agents, and curing conditions were determined based on physical, chemical, and thermal properties of LCEs and curing agents. The thermally cured LCEs at the LC phase exhibited a high thermal conductivity of 0.4 W m^{-1} K^{-1}.

Introduction

Epoxy resin (EP), the most common thermosetting resin, has been used in various industrial applications, caused by its good adhesion, chemical resistance, thermal resistance, and mechanical properties.[1] Generally, uncured EPs only exhibit poor mechanical, chemical, and heat resistance properties. However, EPs are eventually endowed with good properties after treating with suitable reagents to form three-dimensional cross-linked structures.[2] This process is commonly known as curing, and the reagents are known as curatives or curing agents or hardeners. Curing is an exothermic reaction; thus, if it is not controlled, the heat evolved may cause thermal degradation and change the degree of cure. Theoretically, any molecule containing a reactive hydrogen can be used as a curing agent. The reactive hydrogen may react with the glycidyl groups (or epoxide groups) in EP. Typically, amines, acids, acid anhydrides, phenols, alcohols, and thiols are used as curing agents.[3,4] Since curing is conducted by heating, the curing temperature is crucial in determining the mechanical, chemical, and heat resistance of the cured EP. If an insufficient amount of heat is supplied for curing, the network structure is not developed due to incomplete polymerization. Thus, the selection of optimum curing agents, compositions of EP and the curing agent, and curing conditions should be determined on the basis of the physical, chemical, and thermal properties of EP.

Typically, EP exhibits low thermal conductivity, caused by the occurrence of phonon scattering in its three-dimensional cross-linked network structure. The transfer of heat in polymers is well known to occur by the transport of phonon vibrations, which can be expressed in terms of the Debye equation:

$$\lambda = 1/3(C_v u l) \quad (1)$$

Here, λ is the thermal conductivity of the polymer, C_v is the volumetric heat capacity determined from the polymer properties, *e.g.*, density, u is the sound velocity, and l is the mean free path (MFP) of a phonon, which is inversely proportional to the degree of phonon scattering. Although C_v is determined

[a]*Institute of Advanced Composites Materials, Korea Institute of Science and Technology (KIST), Chudong-ro 92, Bondong-eup, Wanju-gun, Jeollabuk-do, 565-905, Korea. E-mail: goh@kist.re.kr; Tel: +82 63 2198141*
[b]*BK21 Plus Haptic Polymer Composite Research Team & Department of Polymer Nano Science and Technology, Chonbuk National University, Jeonju 561-756, Republic of Korea*
[c]*Department of BIN Convergence Technology, Chonbuk National University, 561-756, Republic of Korea*

†Electronic supplementary information (ESI) available: ^{1}H NMR spectra and ^{13}C NMR spectra of all the synthesized compounds, 2-D XRD patterns of DGP30X series, DSC thermograms of mixtures of System 2 and curing agents, and illustration of the curing procedure. See DOI: 10.1039/c7py00243b

‡These authors contributed equally.

by the polymer properties, *e.g.*, density, l is determined by the crystallinity and orientation of the polymer.[5–8] Thus, it is imperative to increase the orientation and crystallinity of the polymer for improving the thermal conductivity of the polymer *via* the increase of the MFP of a phonon (*i.e.*, by decreasing phonon scattering).

Considerable attention has been focused on liquid crystalline epoxy resins (LCEs) as favorable candidates for improving the thermal conductivity of EP because liquid crystal molecules deduce the phonon scattering by the spontaneous orientation of LCE molecules, caused by the excluded volume effect in a domain.[9–16] Indeed, some rod-shaped LCEs exhibit a remarkable thermal conductivity, as high as ~0.4 W m^{-1} K^{-1}; this value is two times greater than that observed for conventional diglycidyl ether of bisphenol A (DGEBA)-type EPs.[16] Furthermore, considerable efforts have been devoted to the development of polymer composites for heat spreading or heat dissipation by incorporating thermal conductive fillers, *e.g.*, graphene oxide,[20] alumina,[21,22] carbon nanotubes,[23] and boron nitride.[16–19] For thermotropic LCEs, curing for developing a network polymer must occur in the range of the LC phase for maintaining LC ordering. If the LC temperature range is not sufficiently wide, the exothermic heat might destroy the LC phase during curing. Furthermore, for practical applications, LCEs are compounded with filler materials, *e.g.*, aluminum oxide, graphene, and boron nitride, for preparing heat-dissipating composite materials. Generally, the thermal conductivity of the polymer composite materials is crucially affected by a percolating network when the critical volumetric concentration of the filler is reached (the percolation threshold).[24] However, if the LC temperature range is not substantially wide, there is a limit to the available filler content, caused by phase separation. As a result, it is difficult to reach the percolation threshold of filler materials; hence, composite materials exhibiting a high thermal conductivity cannot be obtained. Thus, the narrow LC phase range of LCE is a common issue.

In this study, novel LCEs bearing diglycidyl moieties at the side position of the molecule and flexible alkyl chains connecting terminal phenylcyclohexyl (PCH) mesogenic molecules were designed (Scheme 1). By varying the alkyl chain length, several LCE derivatives with the same LC phase were easily synthesized. Furthermore, the LC temperature range of the eutectic mixtures of the newly synthesized LCEs was successfully widened. On account of the wide LC temperature range, a curing agent and curing conditions were easily optimized. The thermal conductivity was also examined using the cured LCE system.

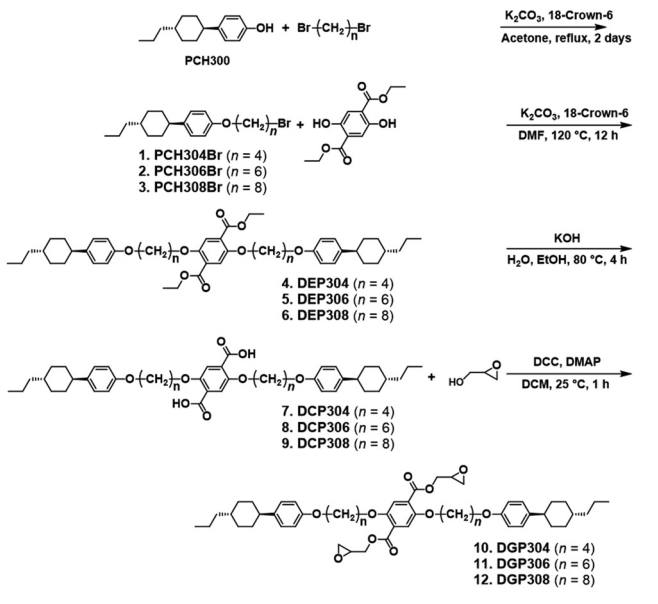

Scheme 1 Synthetic routes for liquid crystalline epoxies bearing diglycidyl moieties at the side position of molecules.

Experimental

Synthesis of liquid crystalline epoxies bearing diglycidyl moieties at the side position of molecules

Novel LCEs were synthesized *via* the substitution of PCH mesogenic moieties into the 2,5 positions of diglycidyl terephthalate. Hereafter, the LCEs with 1-(4-oxybutyloxy)-4-(*trans*-4-*n*-propylcyclohexyl)benzene, 1-(4-oxyhexyloxy)-4-(*trans*-4-*n*-propylcyclohexyl)benzene, and 1-(4-oxyoctyloxy)-4-(*trans*-4-*n*-propylcyclohexyl)benzene moieties are abbreviated as DGP304, DGP306, and DGP308, respectively. Scheme 1 shows the synthetic routes for the compounds of the DGP30X series.

All manipulations were carried out under Ar. Analytical thin-layer chromatography (TLC) was performed on plastic plates coated with 0.25 mm 230–400 mesh silica gel containing a fluorescent indicator (Merck, #1.05715.0009). For silica-gel column chromatography, silica gel 60N (spherical, neutral, particle size 63–219 μm, Merck) was used. All reagents and solvents, except DMF, were of reagent grade and used as received. DMF was purified by passing through a solvent purification system. 4-(*trans*-4-*n*-Propylcyclohexyl)phenol (PCH300) was purchased from Kanto Chemical (Japan). 1,6-Dibromohexane, 18-crown-6, and 4-dimethylaminopyridine (DMAP) were purchased from TCI Co. (Japan). 1,4-Dibromobutane, 1,8-dibromooctane, and *N*,*N*′-dicyclohexylcarbodiimide (DCC) were purchased from Alfa Aesar Co. (USA). Diethyl 2,5-dihydroxyterephthalate, glycidol, *p*-phenylenediamine (PDA), and alumina (100 mesh) were purchased from Sigma-Aldrich Co. (USA). K_2CO_3, KOH, acetone, ethanol, THF, and DCM were purchased from Daejung Chemical Co. (Korea). Diglycidyl ether of bisphenol-A (DGEBA)-type EP (YD-128) was purchased from Kukdo Chemical Co. (Korea). Crystalline EP (SE-400H) was purchased from Shin-A T&C (Korea).

PCH306Br, (2). PCH306Br was synthesized according to a previously reported procedure.[25] In a 500 mL three-neck round-bottom flask, K_2CO_3 (8.3 g, 60.1 mmol), 18-crown-6 (0.8 g, 3.0 mmol), and 1,6-dibromohexane (14.6 g, 9.2 mL, 60.0 mmol) were added to acetone (30 mL), and then a solution of PCH300 (10.9 g, 60 mmol) in acetone (200 mL) was

slowly added to the mixture *via* a dropping funnel. The mixture was stirred at 60 °C for 2 days. After confirming the complete conversion of PCH300 by TLC, the reaction mixture was filtered to eliminate salts, concentrated to ~50 mL, and then poured into MeOH (1 L), affording a precipitate. This precipitate was filtered, washed with deionized water, and dried in a vacuum oven to afford the final product PCH306Br (13.3 g, 35.0 mmol, 70% yield) as a colorless oil, which immediately changed to needle-type crystals. The product was directly used in the next step without further purification. ^{1}H NMR (600 MHz, $CDCl_3$) δ 7.11 (d, 2H, J = 3.0 Hz), 6.83 (d, 2H, J = 3.0 Hz), 3.94 (t, 2H, J = 3.0 Hz), 3.43 (t, 2H, J = 3.0 Hz), 2.40 (m, 1H), 2.0–0.8 (m, 24H). ^{13}C NMR (120 MHz, $CDCl_3$) δ 157.1, 140.0, 127.5, 114.2, 67.6, 43.7, 39.7, 37.0, 34.5, 33.8, 33.6, 32.7, 29.1, 27.9, 25.3, 20.0, 14.4. Other compounds of the PCH30XBr series (PCH304Br and PCH308Br) were also synthesized by the same procedure.

DEP306, (5). In a 500 mL two-neck round-bottom flask, PCH306Br (13.3 g, 35.0 mmol), K_2CO_3 (2.5 g, 18.1 mmol), 18-crown-6 (0.5 g, 1.9 mmol), and diethyl 2,5-dihydroxyterephthalate (4.6 g, 18.1 mmol) were added to anhydrous DMF (170 mL). Second, the mixture was stirred at 120 °C for 12 h. After confirming the complete conversion of PCH306Br by ^{1}H NMR, DMF in the reaction mixture was removed by rotary evaporation, and the remaining reaction mixture was extracted using DCM. The organic layer was washed with H_2O and brine, dried over anhydrous Na_2SO_4, and purified by silica-gel column chromatography using DCM as the eluent (R_f = 0.6) to afford the final product DEP306 (14.5 g, 17.0 mmol, 94% yield) as a colorless solid. ^{1}H NMR (600 MHz, $CDCl_3$) δ 7.36 (s, 2H), 7.12 (d, 4H, J = 3.0 Hz), 6.84 (d, 4H, J = 3.0 Hz), 4.38 (dd, 4H, J = 3.0, 6.0 Hz), 4.03 (t, 4H, J = 3.0 Hz), 3.95 (t, 4H, J = 3.0 Hz), 2.40 (m, 2H), 2.0–0.8 (m, 54H). ^{13}C NMR (120 MHz, $CDCl_3$) δ 166.0, 157.1, 151.7, 139.9, 127.5, 124.6, 116.5, 114.2, 69.6, 67.7, 61.2, 43.7, 39.7, 37.0, 34.5, 33.6, 29.3, 29.2, 25.8, 25.7, 20.0, 14.4, 14.3. Other compounds from the DEP30X series (DEP304 and DEP308) were also synthesized by the same procedure.

DCP306, (8). In a 500 mL round-bottom flask, DEP306 (14.5 g, 17.0 mmol) and excess KOH (53.1 g, 0.95 mol) were added to a mixed solvent system comprising EtOH (40 mL), THF (20 mL), and deionized H_2O (80 mL). Then, the mixture was stirred at 80 °C for 4 h. After confirming the complete conversion of DEP306 by TLC, the reaction mixture was cooled to 0 °C and acidified with aq. HCl (35%), affording a precipitate. The precipitate was filtered and dried in a vacuum oven (60 °C), affording the final product DCP306 (13.6 g, 17.0 mmol, 99% yield) as a colorless solid. ^{1}H NMR (600 MHz, $CDCl_3$) δ 11.09 (br, 2H), 7.84 (s, 2H), 7.11 (d, 4H, J = 3.0 Hz), 6.82 (d, 4H, J = 3.0 Hz), 4.29 (t, 4H, J = 3.0 Hz), 3.94 (t, 4H, J = 3.0 Hz), 2.39 (m, 2H), 2.0–0.8 (m, 48H). ^{13}C NMR (120 MHz, $CDCl_3$) δ 164.1, 157.0, 151.7, 140.1, 127.6, 122.8, 117.4, 114.2, 71.0, 67.5, 43.7, 39.7, 37.0, 34.5, 33.6, 29.1, 28.8, 25.8, 25.7, 25.6, 20.0, 14.4. Other compounds from the DCP30X series (DCP304 and DCP308) were also synthesized by the same procedure.

DGP306, (11). In a 500 mL two-neck round-bottom flask, DCP306 (13.6 g, 17.0 mmol) was suspended in DCM (360 mL), and the suspension was cooled to 0 °C. Then, DMAP (0.3 g, 2.5 mmol), glycidol (10.3 g, 8.8 mL, 0.16 mol), and DCC (22.7 g, 0.11 mol) were added to the reaction mixture. The mixture was stirred at 25 °C for 2 h. After confirming the complete conversion of DCP306 by ^{1}H NMR, the reaction mixture was extracted using DCM. The organic layer was washed with brine, dried over anhydrous Na_2SO_4, and purified by silica-gel column chromatography using DCM as the eluent (R_f = 0.6) to afford the final product DGP306 (10.9 g, 12.0 mmol, 71% yield) as a colorless solid, which was further purified by recrystallization from $CHCl_3$/hexane to obtain a pure compound. ^{1}H NMR (600 MHz, $CDCl_3$) δ 7.37 (s, 2H), 7.08 (d, 4H, J = 3.0 Hz), 6.81 (d, 4H, J = 3.0 Hz), 4.60 (d, 2H, J = 3.0 Hz), 4.16 (dd, 2H, J = 3.0, 6.0 Hz), 4.02 (t, 4H, J = 3.0 Hz), 3.93 (t, 4H, J = 3.0 Hz), 2.39 (m, 2H), 2.0–0.8 (m, 48H). ^{13}C NMR (120 MHz, $CDCl_3$) δ 166.0, 157.1, 151.7, 139.9, 127.5, 124.6, 116.5, 114.2, 69.6, 67.7, 61.2, 43.7, 39.7, 37.0, 34.5, 33.6, 29.3, 29.2, 25.8, 25.7, 20.0, 14.4, 14.3. Other compounds from the DGP30X series (DGP304 and DGP308) were also synthesized by the same procedure.

The structure of the synthesized LC epoxy was determined by ^{1}H NMR and ^{13}C NMR in $CDCl_3$ (NMR, Agilent, solution-state NMR 600 MHz spectrometer). The thermal properties of DGP30X and the cured resin were characterized by differential scanning calorimetry (DSC, Q20, TA Instruments, Inc.) at heating and cooling flow rates of 3 °C min^{-1}. The mesomorphic properties of the synthesized LCE and a mixture of LCEs were evaluated by polarized optical microscopy (POM, ZEISS, AXIO Imager A2m microscope stand), 2D X-ray diffraction (2D-XRD, Bruker, D8 discover with GADDS), and DSC. Thermal conductivity was measured by the transient plane source method (Hot-disk AB, TPS-2500s). Disk-shaped samples with a diameter of approximately 2 cm and a thickness of 2 mm were covered on a thin layer between both sides.

Results and discussion

Mesomorphic properties of DGP30Xs

The mesomorphic properties of DGP30Xs were investigated by POM, DSC, and XRD measurements. Fig. 1a, c, and e show DSC data for DGP304, DGP306, and DGP308, respectively. The phase transition temperatures of DGP304 were K → 146 °C (3 J g^{-1}) → S_A → 154 °C (95 J g^{-1}) → I and I → 102 °C (95 J g^{-1}) → S_A → 88 °C (1 J g^{-1}) → K for heating and cooling processes, respectively (Fig. 1a). Besides, the phase transition temperatures of DGP306 were K → 119 °C (1 J g^{-1}) → S_A → 124 °C (78 J g^{-1}) → I and I → 94 °C (76 J g^{-1}) → S_A → 89 °C (1 J g^{-1}) → K for heating and cooling processes, respectively (Fig. 1c). Furthermore, the phase transition temperatures of DGP308 were K → 77 °C (1 J g^{-1}) → S_A → 89 °C (32 J g^{-1}) → I and I → 74 °C (30 J g^{-1}) → S_A → 19 °C (2 J g^{-1}) → K for heating and cooling processes, respectively (Fig. 1e). Here, K, S_A, and I denote the crystal, highly ordered smectic phase, and isotropic phases, respectively, and the enthalpy changes associated with the phase transitions are shown

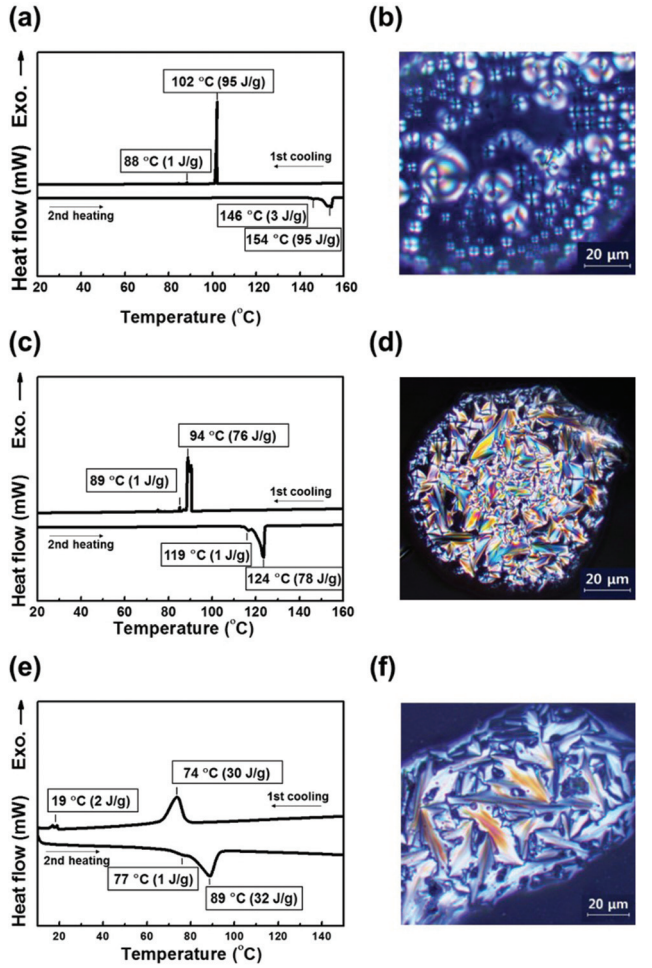

Fig. 1 DSC thermograms of liquid crystalline epoxies, (a) DGP304, (b) DGP306, and (c) DGP308 and POM photographs of (d) DGP304 at 100 °C, (e) DGP306 at 95 °C, and (f) DGP308 at 60 °C on the 1st cooling.

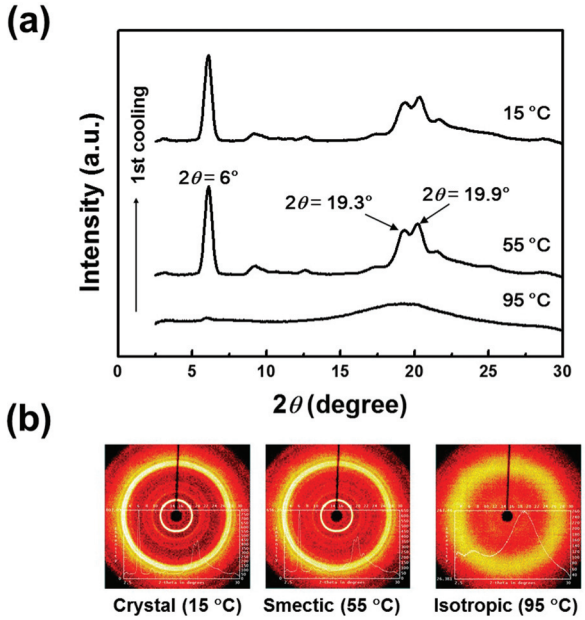

(c)

Peak number	1	2	3
2θ [degree]	6.0	19.3	19.9
d-spacing [Å]	44.1 (*n* = 3)	4.6	4.5
Assigned with	Long axis	Intermolecular distance	Intermolecular distance

Fig. 2 (a) XRD profiles of DGP308 at 15, 55, and 95 °C on the 1st cooling and (b) 2D XRD patterns of DGP308 at 15, 55, and 95 °C. (c) Table of the calculated *d*-spacing values for DGP308 from the XRD results at 55 °C.

within parenthesis. All DGP30Xs exhibited a stable enantiotropic highly ordered smectic phase on heating and cooling. Droplet (Fig. 1b) and fan-shaped textures (Fig. 1d and f) were observed in the POM photographs of DGP304, DGP306, and DGP308, which are characteristic of smectic phases at 100, 95, and 60 °C in the cooling process, respectively.

The XRD measurement of DGP308 was performed during cooling (Fig. 2). At 55 °C, a broad diffraction peak was observed in the large-angle region (2θ = 19.3–19.9°), corresponding to the LC intermolecular distance of 4.5–4.6 Å as a result of the π–π stacking orientation of the mesogenic group. A sharp diffraction peak in the small-angle region (2θ = 6°) corresponded to an interlayer distance of 44.1 Å. This value is consistent with the molecular length of DGP308 (l = 48 Å). Hence, the LC phase of DGP308 at 55 °C can be assigned to the highly ordered smectic phase. Furthermore, those of DGP304 and DGP306 can also be assigned to the S_A phase. Details of DGP304 and DGP306 are described in the ESI (Fig. S12 and S13†).

Eutectic mixtures of DGP30Xs and their mesomorphic properties

Notably, from the viewpoint of the thermal curing of thermotropic LCEs, curing has to occur in an LC phase temperature range for maintaining the orientational ordering of cured LCE. Thus, the limitation of the available temperature range of thermotropic LCE has always been an issue. Besides, the thermal disruption of LCE molecules needs to be minimized, and the ordering needs to be maintained by exothermic curing. Although each DGP30X exhibited a stable enantiotropic S_A phase, the LC phase temperature range was very narrow, less than 10 °C. This temperature range is not suitable for EP curing because the exothermal heat evolved during curing can destroy the LC phase and transform it into an isotropic one. Hence, a more stable EP system with a wide LC temperature range must be prepared to persist the LC phase during exothermal curing.

Several studies have reported the control of the range of the LC phase.[26–28] Hence, to expand the temperature range of the LC phase, LCE monomers are mixed in a constant ratio. Table 1 summarizes the ratios of the LCE mixture systems.

The phase transition behavior of the mixture systems was confirmed by DSC and POM (Fig. 3). DSC measurements were carried out to investigate the thermal transition behavior of

Table 1 Mixing ratios of liquid crystalline epoxies

System name	Components
System 1	DGP304 : DGP306 = 1 : 1 (mol ratio)
System 2	DGP304 : DGP308 = 1 : 1 (mol ratio)
System 3	DGP306 : DGP308 = 1 : 1 (mol ratio)
System 4	DGP304 : DGP306 : DGP308 = 1 : 1 : 1 (mol ratio)

each system during heating and cooling scans. System 1 exhibited three endothermic peaks at 112, 120, and 144 °C, respectively, with the total enthalpy changes associated with the phase transitions of 73 J g^{-1} in the 2nd heating scan, and two exothermic peaks at 81 and 85 °C, respectively, with the total enthalpy changes of 73 J g^{-1} in the 1st cooling scan (Fig. 3a). System 2 exhibited two endothermic peaks at 98 and 145 °C, respectively, with the total enthalpy changes of 73 J g^{-1} in the 2nd heating scan, and two exothermic peaks at 84 and 99 °C, respectively, with the total enthalpy changes of 74 J g^{-1} in the 1st cooling scan (Fig. 3c). System 3 exhibited three endothermic peaks at 92, 95, and 113 °C, respectively, with the total enthalpy changes of 64 J g^{-1} in the 2nd heating scan, and two exothermic peaks at 36 and 59 °C, respectively, with enthalpy changes of 66 J g^{-1} in the 1st cooling scan (Fig. 3e). System 4 exhibited three endothermic peaks at 90, 112, and 134 °C, respectively, with the total enthalpy changes of 55 J g^{-1} in the 2nd heating scan, and three exothermic peaks at 57, 63, and 67 °C, respectively, with the total enthalpy changes of 55 J g^{-1} (Fig. 3g) in the 1st cooling scan. To investigate the detailed phase transition of all systems, POM images were recorded in the temperature range of the LC phase of each system. From the POM results, all systems exhibit a smectic phase within each temperature range of the LC phase (3b, d, f and h). Interestingly, System 1, System 3, and System 4 exhibited two LC states on heating and cooling. However, System 2 exhibited one stable LC state on heating and cooling. Furthermore, the LC temperature range of System 2 was significantly widened between 98 and 145 °C. This temperature range is sufficiently wide for selecting a curing agent and investigating curing. Thus, curing tests are carried out with System 2. Fig. 4 summarizes the temperature ranges of all DGP30Xs and mixture systems. All systems exhibited a stable enantiotropic liquid crystalline phase on heating and cooling. POM photographs of System 1, System 2, System 3, and System 4 exhibited fan-shaped (Fig. 3b) and schlieren textures (3d, f and h).

To confirm the phase transition of System 2, the XRD measurement was conducted during cooling (Fig. 5). At

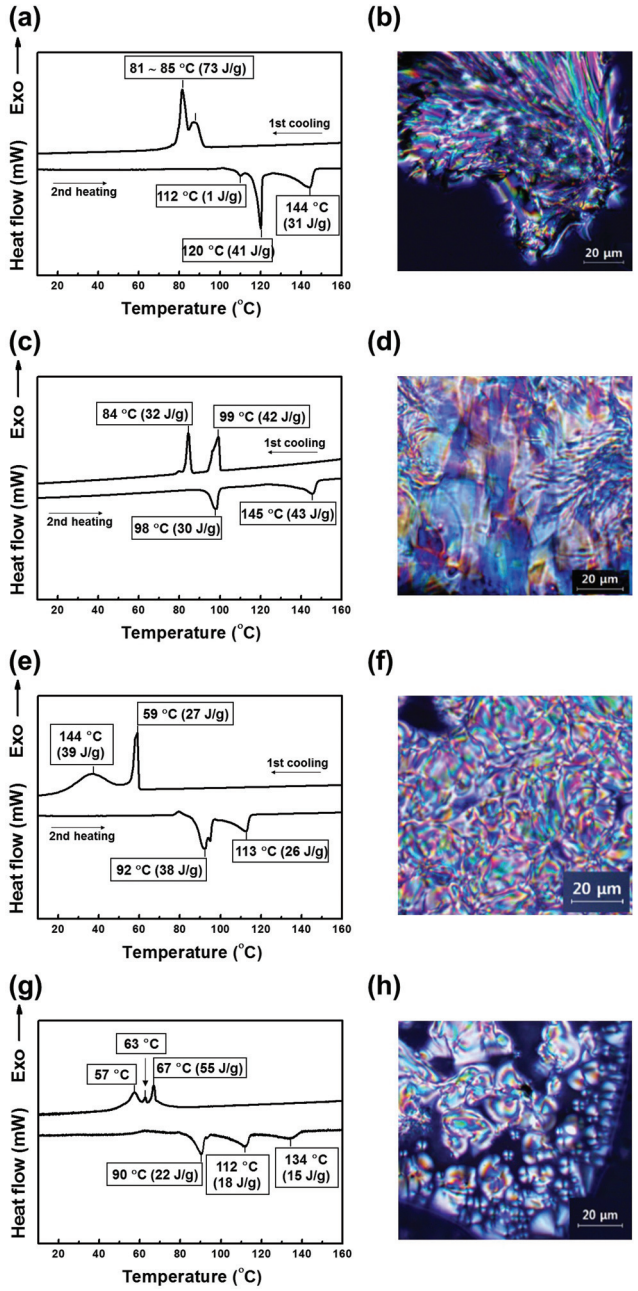

Fig. 3 DSC thermograms of (a) System 1, (c) System 2, (e) System 3, and (g) System 4 and POM photographs of (b) System 1, (d) System 2, (f) System 3, and (g) System 4, respectively.

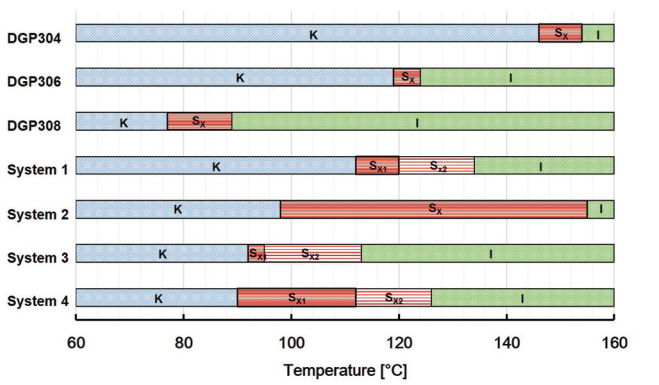

Fig. 4 Phase transition temperatures of DGP304, DGP306, DGP308, System 1, System 2, System 3, and System 4 measured at the 2nd heating rate of 3 °C min^{-1}.

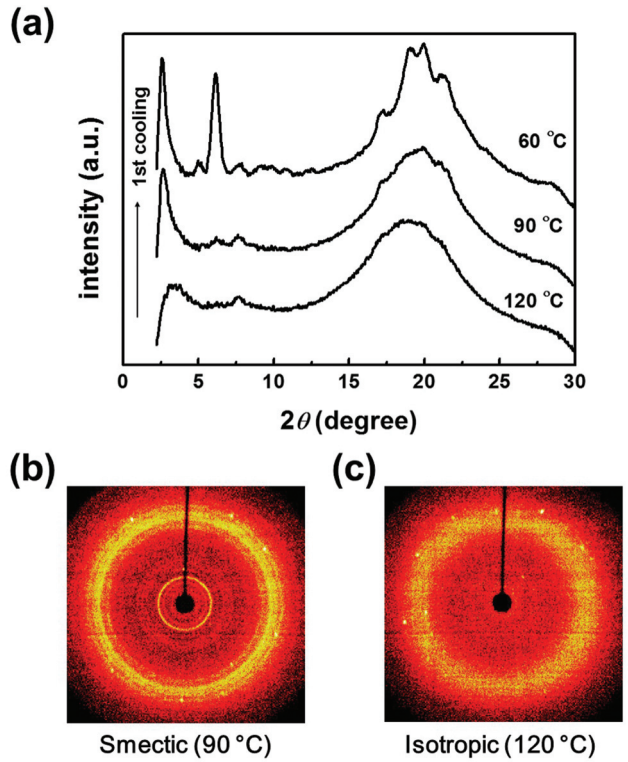

Fig. 5 (a) XRD profiles of System 2 at 60, 90, and 120 °C on the 1st cooling and 2D XRD patterns (b) at 90 °C and (c) at 120 °C.

temperatures greater than 120 °C, a broad, amorphous halo was observed at approximately 2θ = 19.7°, which is a representative XRD pattern of the isotropic phase. In the cooling process, at 90 °C, diffraction peaks were observed at around 2θ = 6.2 and 7.5°, corresponding to the molecular length of DGP304 and DGP308 of System 2, respectively, while the diffractions observed between 2θ = 15 and 22° correspond to the π–π stacking by the mesogenic groups of DGP304 and DGP308. Hence, System 2 at 90 °C can be assigned to the highly ordered smectic phase.

Curing conditions and thermal characterization of the cured liquid crystalline epoxy resin

The selection of a curing agent is just as critical as the selection of resins. As the co-reactive curing agent becomes a part of the network structure, its contribution should be carefully considered.[29] In particular, for LCE, curing must occur in an LC phase temperature range for maintaining the orientational ordering of LCE. Hence, the best curing conditions of LCE can be determined by the optimization of the curing agents and curing temperature as follows. First, a suitable curing agent must be selected, which can facilitate a curing reaction in the LC phase temperature range of LCE (System 2). Second, the most effective curing temperature with the selected curing agent must be determined at the first stage.

To select the curing agent, the thermal behavior in a mixed System 2/curing agent (molar ratio of DGP304 : DGP308 : curing agent = 1 : 1 : 1) was investigated by DSC measurement. Homogeneous mixtures of EP and curing agents were prepared by using a lab mill. Theoretically, the optimum properties of cured EP are observed when an equimolar amount of EP and the curing agent is combined. The EP resin used in this study (DGP304 and DGP308) has two epoxide groups in a molecule. In addition, amine derivatives with two primary amines in a molecule were used as the curing agent. Thus, DGP304, DGP308, and the curing agent are mixed in the same molar ratio. As curing agents, hexamethylenediamine (HMDA), *p*-phenylenediamine (PDA), and 4,4′-diaminodiphenylsulfone (DDS), were used, and curing can occur at *ca.* 100, 150, and 200 °C, respectively. Fig. 6 shows DSC thermograms for mixtures of System 2/curing agents (DDS, PDA, HMDA) in the 1st heating scan. The mixed System 2/DDS exhibited two endothermic peaks at around 92 and 133 °C, respectively, corresponding to the LC phase transition, while the exothermic peak corresponding to the crosslinking reaction was not observed. This result implied that curing occurs in the isotropic state. For System 2/PDA, the LC phase range changed between 91 and 125 °C, and curing started from 105 °C, with a peak top observed at 150 °C. This result indicated that curing occurs in an LC phase temperature range of System 2 and PDA. In contrast, for the mixed System 2/HMPA, an exothermic peak was observed from 63 to 140 °C. This result indicated that curing starts before the LC phase range from 90 to 120 °C. From the above DSC results, the optimal curing agent for System 2 is confirmed to be PDA.

To determine the most effective curing temperature with the selected curing agent PDA, isothermal DSC thermograms of System 2/PDA were recorded at three temperatures of the LC phase temperature range, 105, 115, and 125 °C, respectively (Fig. 7). In Fig. 7a, the initial slope of curing was steeper, and the total enthalpy was greater at 125 °C (141 J g^{-1}) than that at 115 °C (106 J g^{-1}). Furthermore, curing was accomplished within 30 min at 125 °C, but it was completed in approximately 60 min at 115 °C. Curing in the LC phase is possibly

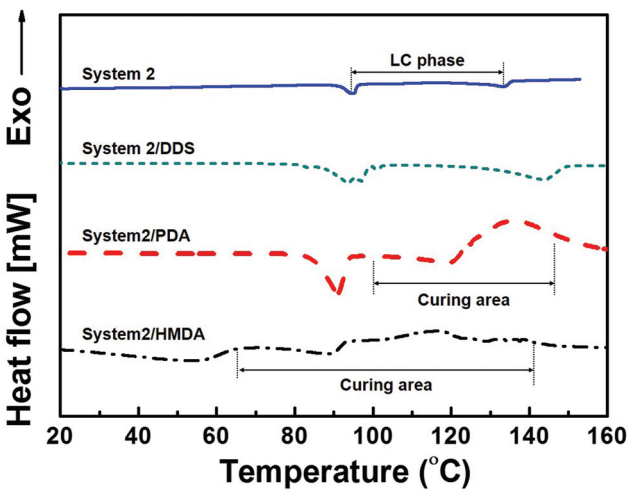

Fig. 6 DSC thermograms of System 2, System 2/DDS mixture, System 2/PDA mixture, and System 2/HMDA mixture on the 1st heating.

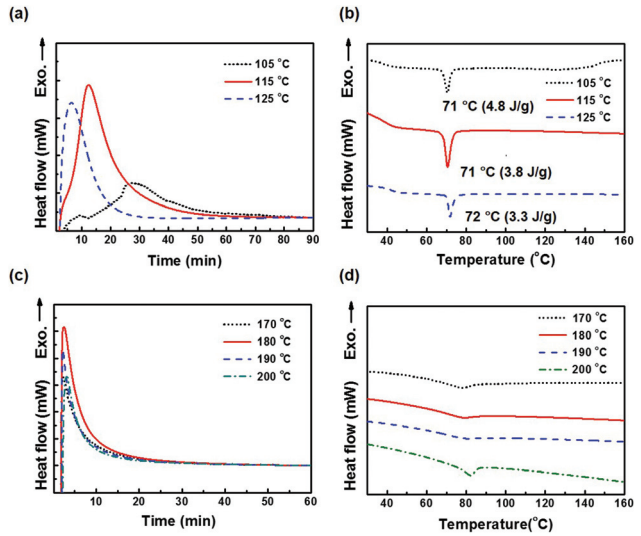

Fig. 7 DSC thermograms for mixtures of System 2 and PDA; (a) isothermal heating for precuring, (b) heating scan after precuring, (c) isothermal heating for post-curing (pre-cured at 125 °C, 60 min), and (d) heating scan after post-curing.

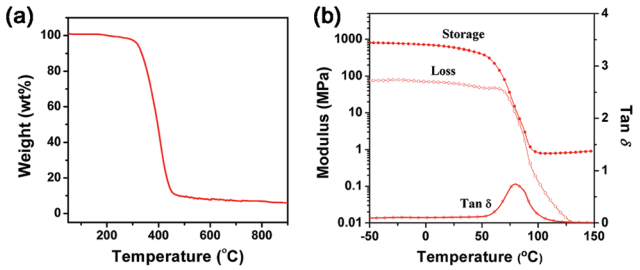

Fig. 8 (a) TGA (heating rate: 10 °C min^{-1}, under an argon atmosphere) and (b) DMA (heating rate: 3 °C min^{-1}, under an air atmosphere, 1 Hz) curves of the cured System 2.

accelerated because of the easy flow of the molecules in the mesophase. After the first curing reaction at 105, 115, and 125 °C, the DSC measurement was conducted to evaluate the thermal properties of cured EP (Fig. 7b). Clear melting was observed in three cured EP samples at around 70 °C. On account of the high curing rate, the lowest total endothermic enthalpy of 3.3 J g^{-1} was observed at 125 °C. Cured EP at 125 °C exhibited a robust solid state. To increase the cross-linking reaction, the post-cure condition with pre-cured EP was examined by isothermal DSC thermograms at 170, 180, 190, and 200 °C. The maximum curing rate (Fig. 7c) and the minimum endothermic enthalpy (Fig. 7d) were observed at 180 °C. Thus, the optimal post-cure temperature is confirmed to be 180 °C.

The fabrication of LCE is as follows. Because LCEs exhibit a crystalline phase up to LC transition, LCEs (System 2) were directly blended with the curing agent PDA as it is a solid powder. System 2 and PDA were each pulverized using a hammer mill (Polymix, PX-MFC 90 D) at 500 rpm. Next, fine powders of System 2 and PDA were mixed together using a mixer (Thinky, SR-500) at 2000 rpm for 3 min, affording a homogeneous mixture without phase separation. The obtained powder mixture was inserted in an SUS mold (inner diameter: 20 mm, thickness: 2 mm), and it was pre-cured under a pressure of 5 MPa using a heating press (Ocean Science, COAD.1006c) at 125 °C for 30 min, followed by post-curing in a vacuum oven at 180 °C for 30 min (Fig. S15†). After pre-curing, the completely cured sample was cut and appropriately polished (diameter 20 mm, thickness 2 mm) to evaluate the thermal conductivity.

The thermal and thermomechanical properties of cured System 2 were investigated by TGA and DMA measurements. Fig. 8 shows the TGA and DMA curves. The decomposition temperatures at 5% weight loss ($T_{d,5\%}$) and 10% weight loss ($T_{d,10\%}$) were 319 °C and 335 °C, respectively. These values are similar to those of ordinary EP, indicating that LCE exhibits sufficient thermal stability for general applications. In addition, the glass transition temperature (T_g) was calculated from the peak top of tan δ, and the value was the same as that obtained from the DSC measurement.

The thermal conductivities of the cured LCEs were measured by the transient plane source method according to the ISO standard 22007-2.[30] Notably, the laser flash method is not suitable for organic materials with a relatively low thermal conductivity. Because of a short irradiation time, the temperature increase of the rear side of the specimen cannot be sufficiently attainable, consequently leading to a considerable error.[31,32] On the other hand, the transient plane source method is appropriate for the organic specimen, covering a wide range of thermal conductivity values (0.01–500 W m^{-1} K^{-1}).[33,34] Table 2 summarizes the measured values, corresponding to the average values obtained from the measurement of the three samples. The thermal conductivities of non-liquid crystalline DGEBA-type epoxy/PDA and biphenyl-type crystalline epoxy/PDA, serving as references to the LCE, were evaluated (Scheme 2).

The thermal conductivities of System 2 (LCE)/PDA, DGEBA/PDA, and crystalline EP/PDA were 0.4, 0.2, and 0.33 W m^{-1} K^{-1}, respectively. Interestingly, the thermal conductivity of cured System 2 was greater than that of crystalline EP/PDA. This result possibly indicated that the liquid crystallinity of LCE could effectively enhance the MFP of phonon vibration, resulting in high thermal conductivity.

As a result, the LCEs prepared herein exhibit higher thermal conductivity as compared with that of conventional

Table 2 Curing conditions and thermal conductivities of System 2, DGEBA, and crystalline epoxy cured by a PDA hardener, respectively

Epoxy type	Curing conditions		Thermal conductivity
System 2	Pre-cure	125 °C, 30 min	0.4 W m^{-1} K^{-1}
	Post-cure	180 °C, 30 min	
DGEBA	Pre-cure	70 °C, 2 h	0.20 W m^{-1} K^{-1}
	Post-cure	130 °C, 2 h	
Crystalline	Pre-cure	110 °C, 2 h	0.33 W m^{-1} K^{-1}
	Post-cure	140 °C, 2 h	

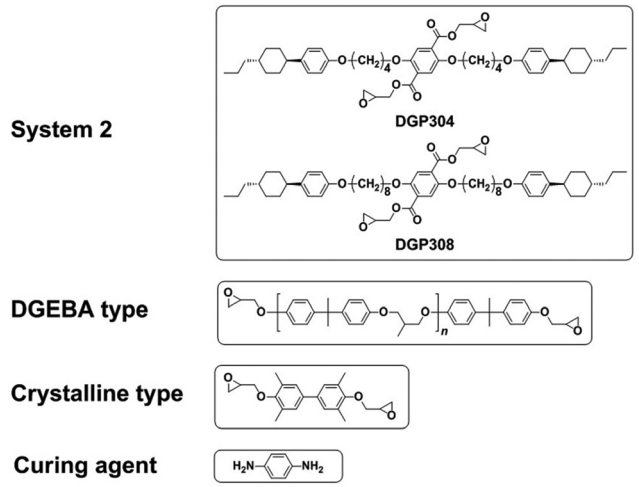

Scheme 2 Molecular structures of System 2, DGEBA type epoxy, crystalline type epoxy, and curing agent PDA.

LCEs.[22] This is a crucial result in this study. The main reason for developing LCEs is to improve thermal conductivity. From the viewpoint of molecular design, to maintain the orientation of LCE molecules after thermal curing, novel LCEs bearing diglycidyl moieties at the side position of the molecule were designed (Fig. 9) because thus far, conventional LCEs contain glycidyl moieties at the ends of the rod-shaped LC molecule, which induce amorphous network structures. Such conventional LCEs are classified as "end type epoxy". When such epoxy compounds are subjected to curing with amine derivatives, the ordered structure of LCEs is disrupted because of the dihedral angle between the C–N–C covalent bond. From the three-dimensional description of the two cured epoxies, which contain glycidyl moieties at the ends (Fig. 9a) and at the side position of the rod-shaped LC molecule (Fig. 9b), respectively, the intermolecular distance of the LC moieties at the side position was more perfectly maintained (Fig. 9b). Hence, "side type epoxy", *i.e.*, the new type of LCEs prepared herein, demonstrates potential as alternatives to prevent the reduction of molecular orientation during curing and improve thermal conduction properties.

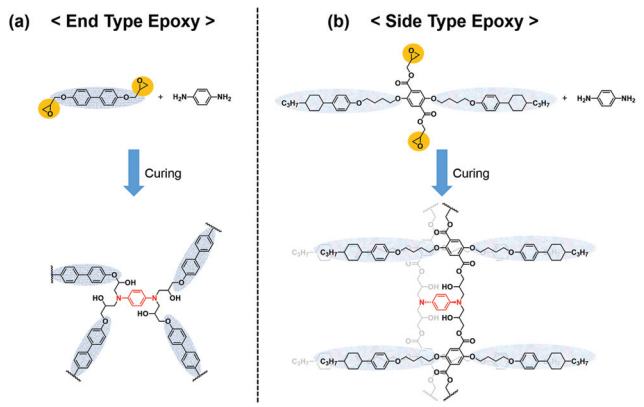

Fig. 9 The proposed mechanism: advantages of side type epoxy for thermal conducting from a viewpoint of molecular alignment.

Conclusions

Three novel liquid crystalline epoxies (LCEs) were synthesized *via* the substitution of phenylcyclohexyl (PCH) mesogenic moieties into the 2,5 positions of diglycidyl terephthalate *via* a flexible alkyl chain. All of the LCE derivatives exhibited an enantiotropic highly ordered smectic phase on heating and cooling. Although the LC phase temperature range of each LCE was narrow, the eutectic mixtures of highly ordered smectic LCEs exhibited a highly ordered smectic phase with a wide temperature range of 98–145 °C. In fact, this sufficiently wide LC temperature range of LCEs permitted the examination and selection of optimum curing agents and curing conditions. In reality, the optimum curing agent was determined on the basis of physical, chemical, and thermal properties of LCEs and curing agents. The thermally cured LCEs at the LC phase exhibited the highest thermal conductivity of 0.4 W m^{-1} K^{-1}. This value is greater than that of typical non-liquid crystalline diglycidyl ethers of bisphenol A (DGEBA)-type epoxy resin (0.20 W m^{-1} K^{-1}). The outstanding thermal conductivity of cured LCEs is possibly related to the deduction of phonon scattering induced by the spontaneous orientation of LCE molecules, caused by the excluded volume effect in a domain. The newly developed LCEs exhibiting outstanding thermal conductivity and an excellent wide liquid crystalline temperature range can be applied as heat-dissipating composite materials in electronic and display devices.

Acknowledgements

This research was supported by a grant from the Korea Institute of Science and Technology (KIST) Institutional program (2Z04750 and 2Z05020). This research was also supported by the Materials and Components Technology Development Program of MOTIE/KEIT, Republic of Korea (10076464, Development of lightweight and high heat dissipating bio-inspired composites for printed circuit boad with thermal conductivity of 20 W/mK.

References

1 L. A. Pilato and M. J. Michno, in *Advanced composite materials*, Springer Science & Business Media, 1994, pp. 11–17.
2 J. Yu, J. Jung, Y. Choi, J. Choi, J. Yu, J. Lee, N. You and M. Goh, *Polym. Chem.*, 2016, **7**, 36–43.
3 D. Zhou, M. Lu, L. Liang, T. Shen and W. Xiao, *Polym. Eng. Sci.*, 2012, **52**, 1375–1382.
4 J. Gao, L. Juo and Y. Du, *J. Appl. Polym. Sci.*, 2012, **125**, 3329–3334.

5 D. Hansen and G. A. Bernier, *Polym. Eng. Sci.*, 1972, **12**, 204–208.
6 M. Akatsuka and Y. Takezawa, *J. Appl. Polym. Sci.*, 2003, **89**, 2464–2467.
7 B. Y. Cao, Y. W. Li, J. Koing, H. Chen, Y. Xu, K. L. Yung and A. Cai, *Polymer*, 2011, **52**, 1711–1715.
8 G. Kim, D. Lee, A. Shanker, L. Shao, M. S. Kwon, D. Gidley, J. Kim and K. P. Pipe, *Nat. Mater.*, 2015, **14**, 295–300.
9 L. C. Chien, C. Lin, D. S. Fredley and J. W. McCargar, *Macromolecules*, 1992, **25**, 133–137.
10 J. J. Mallon and P. M. Adams, *J. Polym. Sci., Part A: Polym. Chem.*, 1993, **31**, 2249–2260.
11 C. Ortiz, R. Kim, E. Rodighiero, C. K. Ober and E. J. Kramer, *Macromolecules*, 1998, **31**, 4074–4088.
12 J. Y. Lee, J. Jang, S. M. Hong, S. S. Hwang and K. U. Kim, *Polymer*, 1999, **40**, 3197–3202.
13 M. Harada, M. Ochi, M. Tobita, T. Kimura, T. Ishigaki, N. Shimoyama and H. Aoki, *J. Polym. Sci., Part B: Polym. Phys.*, 2003, **41**, 1739–1743.
14 Y. Li, P. Badrinarayanan and M. R. Kessler, *Polymer*, 2013, **54**, 3017–3025.
15 Y. Li and M. R. Kessler, *Polymer*, 2013, **54**, 5741–5746.
16 M. Harada, N. Hamaura, M. Ochi and Y. Agari, *Composites, Part B*, 2013, **55**, 306–313.
17 K. C. Yung and H. Liem, *J. Appl. Polym. Sci.*, 2007, **106**, 3587–3591.
18 K. Kim, H. Ju and J. Kim, *Polymer*, 2016, **91**, 74–80.
19 F. Wang, Y. Yao, X. Zeng, T. Huang, R. Sun, J. Xu and C. P. Wong, *RSC Adv.*, 2016, **6**, 41630–41636.
20 B. Qi, S. R. Lu, X. E. Xiao, L. L. Pan, F. Z. Tan and J. H. Yu, *eXPRESS Polym. Lett.*, 2014, **8**, 467–479.
21 X. Wu, P. Jiang, Y. Zhou, J. Yu, F. Zhang, L. Dong and Y. Yin, *J. Appl. Polym. Sci.*, 2014, **131**, 40528.
22 H. Yeo, A. Islam, N.-H. You, S. Ahn, M. Goh, J. R. Hahn and S. G. Jang, *Compos. Sci. Technol.*, 2017, **141**, 99–105.
23 M. Abdalla, D. Dean, M. Theodore, J. Fielding, E. Nyairo and G. Price, *Polymer*, 2010, **51**, 1614–1620.
24 D. Stauffer and A. Aharony, in *Introduction to Percolation Theory*, Taylor & Francis, 2nd edn, 1991, pp. 93–121.
25 M. Goh, M. Kyotani and K. Akagi, *J. Am. Chem. Soc.*, 2007, **129**, 8519–8527.
26 I. Gvozdovskyy, *Liq. Cryst.*, 2016, **43**, 1813–1830.
27 K. Tanaka, F. Ishiguro, J. H. Jeon, T. Hiraoka and Y. Chujo, *NPG Asia Mater.*, 2015, **7**, e174.
28 D. S. Hulme and E. P. Raynes, *J. Chem. Soc., Chem. Commun.*, 1974, **3**, 98–99.
29 H. F. Mark, in *Encyclopedia of Polymer Science and Technology, Concise*, John Wiley & Sons, 3rd edn, 2007.
30 S. E. Gustafsson, *Rev. Sci. Instrum.*, 1991, **62**, 797–804.
31 W. N. Dos Santos, P. Mummery and A. Wallwork, *Polym. Test.*, 2005, **24**, 628–634.
32 U. Hammerschmidt, J. Hameury, R. Strnad, E. Turzó-Andras and J. Wu, *Int. J. Thermophys.*, 2015, **36**, 1530–1544.
33 S. A. Al-Ajlan, *Appl. Therm. Eng.*, 2006, **26**, 2184–2191.
34 R. J. Warzoha and A. S. Fleischer, *Int. J. Heat Mass Transfer*, 2014, **71**, 790–807.